ELSEVIER

Journal of Chromatography A, 922 (2001) 139–149

JOURNAL OF CHROMATOGRAPHY A

www.elsevier.com/locate/chroma

Union of capillary high-performance liquid chromatography and microcoil nuclear magnetic resonance spectroscopy applied to the separation and identification of terpenoids

Michael E. Lacey[a,b], Z. Jessica Tan[a,b], Andrew G. Webb[b,c], Jonathan V. Sweedler[a,b,*]

[a]*Department of Chemistry, University of Illinois at Urbana-Champaign, Urbana, IL 61801, USA*
[b]*The Beckman Institute, University of Illinois at Urbana-Champaign, Urbana, IL 61801, USA*
[c]*Department of Electrical and Computer Engineering, University of Illinois at Urbana-Champaign, Urbana, IL 61801, USA*

Received 14 February 2001; received in revised form 23 April 2001; accepted 24 April 2001

Abstract

This paper describes the first coupling of a commercial capillary HPLC system with a diode array spectrophotometric detector and a custom-built nuclear magnetic resonance (NMR) flow microprobe. The eluent from a 3-μm diameter C_{18} HPLC column is linked to a 500 MHz ^{1}H-NMR microcoil probe with an observe volume of 1.1 μl. The separation and structurally-rich detection of a mixture of terpenoids under both isocratic and gradient solvent elution conditions is presented. The lowest limits of detection yet reported for capillary HPLC on-line measurement (i.e., 37 ng for α-pinene) are achieved with this system. The complementary nature of diode array and NMR detection allows stopped-flow data collection from analytes which would otherwise go unnoticed in continuous-flow NMR. Moreover, stopped-flow NMR data is presented for the detection of a trace (sub-nmol) impurity in the sample mixture. Since NMR signals degrade and shift during solvent gradients, flow injection analysis studies are conducted with injected solvent plugs differing in mobile phase composition. The NMR signal degradation accompanying these injections is largely due to the variance in chemical shift with the solvent composition rather than to changes in magnetic susceptibility of the solvent. Characterization of such effects enables the development of improved NMR probes for the coupling of capillary HPLC and NMR.

Keywords: Nuclear magnetic resonance spectroscopy; Capillary liquid chromatography; Microfluidics; Detection, LC; Terpenoids

1. Introduction

As scientists in all disciplines attempt to address increasingly sophisticated questions, there has been a corresponding drive to develop methods of chemical analysis that can provide an unprecedented level of molecular information from a given sample. Within the realm of analytical chemistry, this trend manifests itself both in the creation of novel characterization techniques and in the joining together of established methods [1].

While certain multimode separation and detection combinations such as gas chromatography–mass

*Corresponding author. Department of Chemistry, University of Illinois at Urbana-Champaign, Urbana, IL 61801, USA. Tel.: +1-217-2447-359; fax: +1-217-2448-068.

E-mail address: jsweedle@uiuc.edu (J.V. Sweedler).

0021-9673/01/$ – see front matter
PII: S0021-9673(01)00912-8

spectrometry (GC–MS) and liquid chromatography–MS are relatively commonplace, efforts to expand the scope of suitable analytes and the range of information demand new hyphenated capabilities. We report here the successful integration of a commercial capillary-based HPLC (cHPLC) system [2] with an in-line diode array spectrophotometric detection (DAD) system and a custom-built microcoil nuclear magnetic resonance (NMR) flow microprobe.

In general, MS, infrared (IR) spectroscopy, and NMR spectroscopy are the most commonly used techniques for primary characterization of unknown compounds.

Despite its extensive capabilities in the elucidation of molecular structure and dynamics, NMR spectroscopy suffers from relatively poor mass sensitivity [signal-to-noise (S/N) per unit mass] which arises from the intrinsically low energies of nuclear spin transitions. In fact, NMR trails IR and MS by several orders of magnitude in terms of limits of detection (LODs). During the past several decades, significant improvements in NMR sensitivity have been realized through a variety of approaches including the development of superconducting magnets with increased field strengths, novel methods of polarization transfer [3,4], cryogenic probes [5–7], and reduced-diameter radiofrequency (RF) coils [7–10]. Since mass sensitivity is inversely proportional to RF coil diameter to a first approximation [11], microcoil NMR probes (typically solenoidal RF coils of diameter <1 mm) with observe volumes (V_{obs}) ranging from 5 nl to 1 μl have demonstrated particular promise for mass-limited samples [12,13].

Since the initial demonstrations of HPLC-NMR more than 2 decades ago [14,15], there have been many significant contributions that have accelerated the maturation of this hyphenated technique. With advances in solvent suppression [16,17] and HPLC systems coupled to increasingly powerful magnets [18], analytical-scale HPLC–NMR and its extension to HPLC–NMR–MS have enjoyed widespread use in studies ranging from the classification of natural products [19] to a variety of pharmaceutical analyses [20]. For examination of complex mixtures such as the metabolic products of prospective pharmaceutical candidates or the full complement of chemical messengers within a neuron, successful analytical approaches require the capability to separate and identify components that are frequently present in minute quantities. In an effort to generate the tools needed to accomplish such challenging experiments, the union of small-volume NMR probes with capillary separations has only recently come to fruition. While Wu et al. were the first to link nl-volume NMR detection with both capillary electrophoresis (CE) [21,22] and microbore HPLC [23], Albert and co-workers achieved the initial illustrations of customized cHPLC with NMR detection [24,25] and capillary electrochromatography (CEC)–NMR [26]. Several additional applications of capillary separations coupled to nl-volume NMR detection have demonstrated the utility of the technique both for on-flow analyte identification and for stopped-flow data collection [13,27–29]. Stopped-flow analysis enables improved S/N and even multidimensional experiments for richer structural information.

We discuss here the successful integration of a commercial cHPLC–DAD instrument with a custom-built microcoil NMR probe such that both the chromatography and the detection have been designed to function with microfluidics. In addition to the advantage of reduced solvent consumption (often an important concern when expensive deuterated solvents are employed), this capillary configuration enables more effective chromatographic separation and detection of mass-limited quantities since the analyte concentration in the peak maximum is typically inversely proportional to the square of the column I.D. for a given injected amount [30]. Most past experimental examples in the literature of capillary-scale (<350 μm diameter columns) HPLC–NMR have required solvent splitting in conjunction with standard HPLC pumps to achieve suitable flow-rates, although microbore (350 μm–2 mm diameter columns) HPLC–NMR has been demonstrated without solvent splitting [27]. The cHPLC instrument used here can accurately and reproducibly generate low μl-per-minute flow-rates for both isocratic and gradient elution conditions with flow precision in the nl range for solvent mixtures [2]. As a demonstration of system performance, a mixture of terpenoids is characterized under both isocratic and gradient separation conditions with on-line NMR detection. The complementary nature of the diode array detector allows stopped-flow data collection from analytes which could go unnoticed in con-

tinuous-flow NMR. To illustrate this point, an NMR spectrum is presented for an impurity peak that required signal averaging under stopped-flow conditions.

Terpenoids are commonly found in nature and have a broad range of function in areas as diverse as visual pigments [31], signaling molecules [32], and cell membranes [33]. In addition, the utility of on-line HPLC–NMR has been shown in such experiments as the proper classification of the plant species *Zaluzania grayana* via the elucidation of terpenoid chemistry [34]. The cHPLC–DAD–NMR system described here will further extend these capabilities and enable structural characterization in a variety of areas using markedly lower amounts of sample.

2. Experimental

2.1. Reagents

(1*R*)-(+)-Camphor (98%), (1*R*)-*endo*-(+)-fenchyl alcohol (96%), γ-terpinene (97%), and (1*S*)-(−)-α-pinene (98%) were obtained from Aldrich (Milwaukee, WI, USA). Deuterium oxide (D_2O, 99.9% D), acetonitrile-d_3 (d-ACN, 99.8% D), and acetone-d_6 (99.9% D) were from Cambridge Isotope Labs. (Andover, MA, USA). Acetonitrile (ACN) and cupric sulfate ($CuSO_4 \cdot 5H_2O$) were obtained from Fisher Scientific (Pittsburgh, PA, USA). All reagents were used as received. Water was dispensed from a Milli-Q water purification system (Millipore, Bedford, MA, USA).

2.2. cHPLC–NMR apparatus

A commercial cHPLC system (CapLC system; Waters, Milford, MA, USA) with a 15 cm×0.32 mm C_{18} column (5 μm particles, 300 Å pore size, Symmetry300; Waters) was employed for all the cHPLC–NMR experiments. The CapLC system featured a light-guided flow cell for UV–Vis absorbance detection via a photodiode array [2]. The outlet of the CapLC system was connected to a four-port, 100-nl internal loop sample injection valve (Valco, Houston, TX, USA). When long NMR data acquisitions were necessary, this valve was set to a intermediate position in conjunction with cHPLC pump stoppage to halt the flow when a peak of interest reached the NMR flow cell. The pressure was monitored by the cHPLC instrument and found to be stable with the valve in its mid-position. The outlet of the valve was connected to ~5 m of fused-silica transfer capillary (100 μm I.D.×360 μm O.D.; Polymicro Technologies, Phoenix, AZ, USA). The separations presented here were conducted at ambient temperature and a flow-rate of 3 μl/min.

As described previously [27], the transfer capillary was connected to a 2.3-cm long NMR detection capillary (700 μm I.D.×850 μm O.D.) using polyimide resin (PI-2721; HD Microsystems, Parlin, NJ, USA) according to the manufacturer's processing guidelines. The other end of the NMR detection capillary was affixed via a heat-shrink PTEE/FEP sleeve (Small Parts, Miami Lakes, FL, USA) to a PTFE tube which exited the NMR probe. The microcoil and impedance matching circuitry were fabricated in our laboratory according to previously described procedures [27,35]. A 2.7-mm long solenoidal RF coil was constructed by wrapping 10 turns of polyurethane-coated, flat copper wire (50 μm×225 μm; California Fine Wire, Grover Beach, CA, USA) around a detection capillary (700 μm I.D.×850 μm O.D.) to create an observe volume of ~1.1 μl. A ~3 mm space was allotted between the end of the microcoil and the connection to the transfer capillary to minimize magnetic susceptibility-induced spectral degradation due to the polyimide connection. The microcoil was enclosed by a 10-ml polethylene bottle filled with a perfluorinated liquid for magnetic susceptibility matching purposes. This magnetic susceptibility matching fluid (MF-1, MRM, Savoy, IL, USA) consists of a mixture of perfluorinated organic compounds. The static line width at half-maximum (LW) for this probe was 1.5 Hz. The 90° pulse width was 3.5 μs for a transmitter attenuation of 43 dB on a Varian Inova console.

2.3. cHPLC–NMR separations and flow injection analysis

Terpenoid mixtures containing camphor, fenchyl alcohol, γ-terpinene, and α-pinene were prepared in either d-ACN–D_2O (60:40) or ACN–water (60:40), depending upon the particular experiment. For each of the separations shown here, 2.5 μl of the ter-

penoid mixture was injected onto the column. For the isocratic separation and the stopped-flow NMR acquisition on the selected impurity, the analyte concentrations were as follows: camphor (8 m*M*), fenchyl alcohol (9 m*M*), γ-terpinene (12 m*M*), and α-pinene (15 m*M*). In all other cases, the terpenoids were present at 10 m*M* each. In the isocratic separations, the mobile phase consisted of d-ACN–D_2O (70:30). Under gradient elution conditions, the d-ACN composition increased linearly with time (from 50 to 90% over the course of 30 min, held at 90% d-ACN over the final 10 min of the run).

In addition, to better characterize the NMR signal degradation which seems to accompany many HPLC–NMR injection bands, a series of flow injection analysis (FIA) experiments were performed. For these runs, a programmable syringe pump (PHD 2000; Harvard Apparatus, Holliston, MA, USA) was connected to transfer capillary of the microcoil NMR probe. A series of injections was made with both 200-nl and 3-μl injection loops into a variety of mobile phases. The magnetic susceptibilities of the samples and the mobile phases were measured with a magnetic susceptibility balance that records values to $\pm 0.001 \cdot 10^{-6}$ cgs units (MSB Auto, Alfa Aesar, Ward Hill, MA, USA). The effects on the resonance frequency and line shape of the solvent peaks were monitored after the injections.

2.4. NMR spectroscopy

All NMR experiments were conducted on a Varian Inova 500 MHz (11.7 T) spectrometer with an 89-mm bore. For the cHPLC–NMR experiments, data collection was initiated concurrently with sample injection onto the cHPLC column. Eight transients (NT=8) were acquired with a 65° RF pulse so that one spectrum was collected per 10 s of experimental time [acquisition time per transient (AT)=1.24 s]. For runs under isocratic elution, the spectral width (SW) was 3200 Hz and the number of complex points (NP) was 7936. For gradient elution conditions as well as the analysis of the effect of diffusion on γ-terpinene, the SW was 3800 Hz and NP was 9424. All of these spectra were processed with an exponential line broadening (LB) value of 1.5 Hz and backwards linear prediction (LN) of the first two points (pts) in the free induction decay prior to Fourier transformation to minimize an uneven baseline that arose from the spectral background of the NMR probe. For the stopped-flow acquisition on the selected impurity peak in the terpenoid mixture, the total NMR experimental time was 91 min with AT=1.498 s, NT=3200, SW=5000 Hz, NP=14 976, and a delay (d1)=0.2 s. This spectrum was processed with LB=1 Hz. For this stopped-flow spectrum, a baseline correction was employed to minimize the effect of the probe background; linear prediction was not used since the lower sample amounts relative to the solvent resonances rendered it ineffective. For the FIA, a 90° RF pulse was employed to acquire one spectrum per 5 s with NT=1, AT=1.995 s, SW=2999.2 Hz, NP=11 968, and d1=3 s. The first spectrum of each run was referenced to 1.92 ppm using the d-ACN signal from the solvent. No line broadening was used to process the spectra in the FIA data set. Since all of the experiments were performed in deuterated solvents, the full spectrometer gain could be used without employing solvent suppression techniques.

3. Results and discussion

Despite numerous advances during the past 2 decades in HPLC–NMR, miniaturization of the technique to the capillary scale has encountered challenges that have impeded its development. The cHPLC–DAD–NMR system (Fig. 1) reported here represents an important extension of previous capabilities through the addition of a commercial cHPLC system [2] with microfluidics designed to operate on the capillary scale and which offers a diode array spectrophotometric detector with increased sensitivity for capillary measurements. The combination of diode array detection and HPLC–NMR has demonstrated utility with conventional scale (4.6 mm) separation columns [36]. This relatively simple configuration allows coupling of the cHPLC system with a microcoil NMR flow probe for both on-line and stopped-flow data collection.

With a mobile phase composition of d-ACN–D_2O (70:30) and a flow-rate of 3 μl/min, the UV chromatogram in Fig. 2A shows baseline separation for all four terpenoid analytes as they pass through the flow cell in the cHPLC instrument. Although all

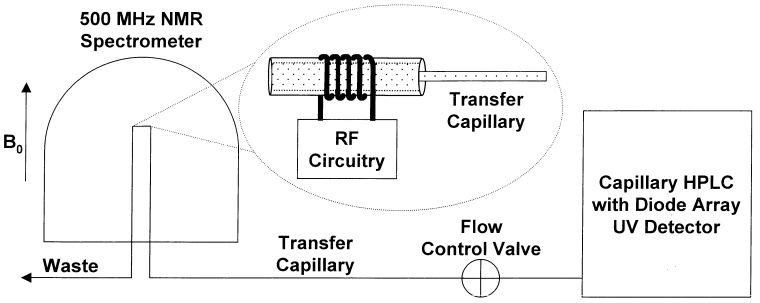

Fig. 1. Schematic of the cHPLC–NMR set-up in which the cHPLC instrument (C_{18} column, 15 cm×0.32 mm) with a diode array UV detector is located ~4 m from the 11.7 T NMR magnet. The flow control valve is used to halt the flow so that peaks of interest can be positioned in the microcoil NMR detection cell (V_{obs}~1.1 μl) for long data acquisitions.

four species are present in approximately equivalent amounts, the UV trace illustrates the dramatically different chromophoric characteristics of these species. While only a single wavelength (λ=244 nm) is shown here, the chromatogram in Fig. 2A is representative of the relative absorptivity of these terpenoids in the 200–400 nm range. One advantage of diode array detection is that a UV–Vis spectrum can be produced for each point in the chromatogram. The on-flow UV and NMR spectra that correspond to α-pinene are illustrated in the inset of Fig. 2A and Fig. 2B, respectively. While the UV spectrum is consistent with an injected α-pinene standard, the much higher information content of the NMR spectrum allows assignment of the peak labeled as 5 in Fig. 2A to α-pinene (and the other peaks in the chromatogram to their corresponding terpenoids).

Gradient elution typically offers faster separations and higher peak capacities, and provides a convenient means of sample preconcentration. As demonstrated by the UV chromatogram (Fig. 3A), the solvent gradient significantly sharpens up the later-eluting peaks (i.e., γ-terpinene and α-pinene). However, despite the improvements in the UV chromatogram, the NMR chromatogram (Fig. 3B) reveals some of the difficulties associated with on-flow data acquisition and solvent gradient HPLC–NMR. As one example, resonances shift as a result of the changing solvent composition. This effect is most apparent in the HOD signal which moves upfield by more than 1 ppm as the mobile phase composition increases from 50% d-ACN to 90% d-ACN over the course of 30 min. Slight upfield shifts in the other analyte resonances are also evident upon closer inspection. The net effect is that, though the analytes are presented to the NMR detector in a more concentrated form, degradation in the lineshape of the resonances prevents full realization of sensitivity gains in terms of S/N. Using the doublet from γ-terpinene at 0.95 ppm, the NMR chromatographic peak width decreases from 130 s (baseline width) for isocratic conditions to 90 s with the solvent gradient. While the integrated area slightly more than doubles for the gradient conditions, the S/N increases by only 8%. Given the overall decrease in spectral resolution under gradient elution, its implementation must be selected judiciously for continuous-flow HPLC–NMR data collection.

In establishing the experimental conditions for continuous-flow HPLC–NMR, one must consider how signal averaging of the NMR data will affect the chromatographic resolution and detection sensitivity in the NMR chromatogram [37]. In some cases, the size of the data files must also be considered. The NMR spectrum presented in Fig. 2B represents the most intense 10-s slice of data for α-pinene collected during the isocratic elution conditions. However, spectra that appear both before and after this slice also contain useful data. In fact, a stacked plot of these spectra (see inset of Fig. 2B) exhibits the chromatographic profile of α-pinene as it passes through the NMR V_{obs}. When NMR data are acquired with relatively good time resolution, the chromatographic peak profile is preserved. Furthermore, spectral addition of relevant slices after completion of the HPLC–NMR run allows one to improve the overall S/N of the NMR spectrum. As one example, slices from the isocratic separation were selected, pro-

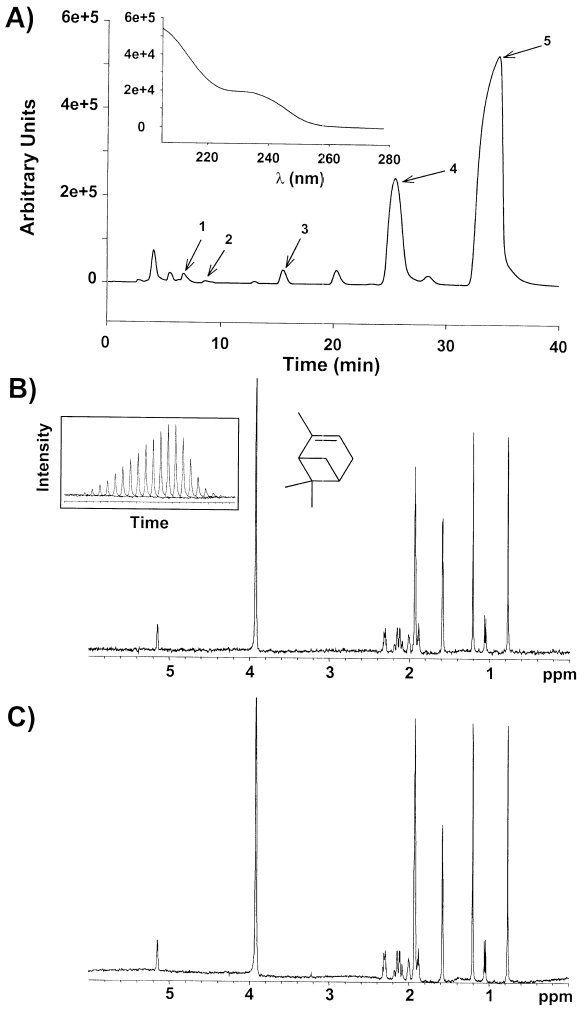

Fig. 2. Isocratic elution cHPLC–NMR of a terpenoid mixture: (A) UV (λ=244 nm) chromatogram with 1=camphor, 2=fenchyl alcohol, 3=impurity, 4=γ-terpinene, 5=α-pinene. Inset: On-flow UV spectrum of α-pinene. (B) On-flow NMR spectrum of α-pinene. Inset: Stacked plot (with no vertical offset) of 20 consecutive on-flow slices, where the region from 1.10 to 1.40 ppm is displayed for each slice. (C) Sum of eight most intense on-flow NMR spectra of α-pinene. ~25 nmol of each analyte injected. Acquisition and processing parameters: SW=3200 Hz, NP=7936, NT=8, AT=1.24 s, total NMR experimental time per spectrum=10 s, LB=1.5 Hz, LN=2 pts.

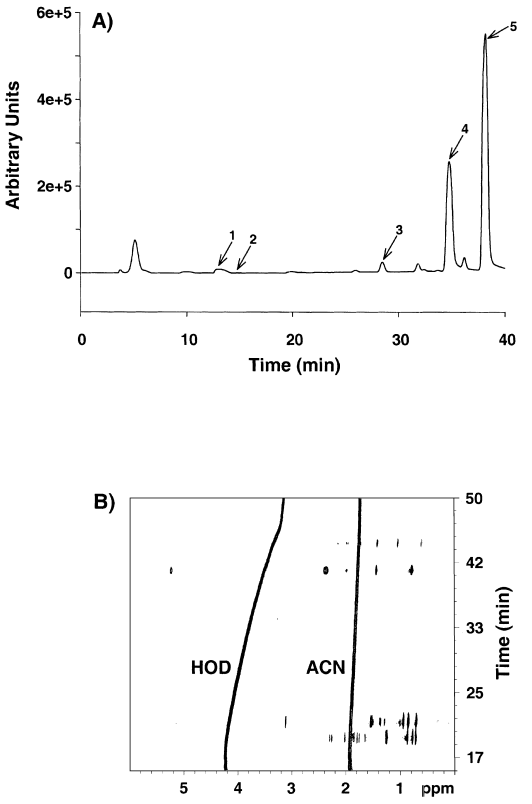

Fig. 3. Gradient elution cHPLC–NMR of a terpenoid mixture: (A) UV (λ=244 nm) chromatogram with labeling as in Fig. 2. (B) NMR chromatogram in which the spectral array is represented as a contour plot. ~25 nmol of each analyte injected. Acquisition and processing conditions as in Fig. 2 except SW=3800 Hz, NP=9424. The residual protonated water and acetonitrile in the mobile phase are labeled as HOD and ACN, respectively.

cessed, and added together for α-pinene. The resultant spectrum is shown in Fig. 2C. The S/N increased from 159 for the resonance at 0.77 ppm in the single slice shown in Fig. 2B to 406 for the sum (Fig. 2C) of seven additional spectra surrounding the most intense slice. Adding free induction decays (unprocessed time domain data) yielded equivalent results. Despite performing the NMR data collection in an unlocked mode, the full width at half maximum of the signal at 0.77 ppm (after 1.5 Hz line broadening) increased only from 3.07 Hz to 3.19 Hz. Clearly, spectral addition represents an attractive approach to improve NMR S/N via a simple processing step while preserving chromatographic resolution for isocratic separations. Improvements in S/N for gradient elution would not be as substantial due to the shifting resonances with varying solvent composition. For an LOD defined as the amount or concentration that yields a S/N=3, LODs for α-pinene improve from 0.69 nmol (93 ng) to 0.27 nmol

(37 ng) as a result of spectral addition. The LODs achievable with this cHPLC–DAD–NMR system represent the best reported to date for on-line cHPLC–NMR. Although not shown here, injections of terpenoid mixtures with 5 nmol of each component were readily detected with sensitivities in accordance to values extrapolated from the data presented here. Of course, NMR spectra for structural elucidation of unknown species require a signal-to-noise ratio above the LOD (e.g., $S/N>10$).

In both the isocratic and the gradient separations, an impurity peak (labeled ''3'' in Figs. 2A and 3A) was visible in the UV chromatograms but did not appear in the on-flow NMR data. To position this analyte within the NMR V_{obs}, the delay time between the UV–Vis flow cell and the NMR flow cell was determined from the terpenoid peaks that had previously eluted during the separation. At the calculated juncture, the in-line flow control valve (Fig. 1) was switched to an intermediate position to halt the flow of the mobile phase. Signal averaging for 91 min under stopped-flow conditions generated the spectrum shown in Fig. 4. The two largest peaks at ~3.9 ppm and 1.92 ppm are due to residual protonated species from the deuterated water and acetonitrile, respectively. The broad signal that spans the region from 1.2 to 1.6 ppm is generated from residual protons in the fluid (MF-1) used for magnetic susceptibility matching. Through injection of samples prepared from the individual terpenoids, it was determined that the impurity most likely arose from a synthesis by-product or decomposition product of γ-terpinene. While it is difficult to calculate exactly how much material is present in this impurity peak, the injected amount is certainly below 1 nanomole given the S/N in the spectrum in Fig. 4 and the sensitivity of this microcoil probe as determined with standard solutions. Although there are definitely some characteristic features (such as the quartet at 7.1 ppm), this one-pulse ^{1}H-NMR spectrum must be evaluated within the context of additional data from other experiments in order to provide definitive structural elucidation of this compound. A combination of fraction collection and on-line mass spectrometric capabilities would facilitate further study of analytes with unknown structure. Nonetheless, the utility of the cHPLC–DAD–NMR system is evident from the complementary nature of the detectors. As the UV chromatograms in Figs. 2 and 3 illustrate, the impurity peak generates a larger response at 244 nm than either camphor or fenchyl alcohol. The combination of the capability to examine the UV–Vis wavelength range from 200 to 800 nm and the near universal proton detection capability of NMR improves the efficiency with which compounds are observed, compared to either detector individually.

Since relatively low sensitivity makes NMR detection of microseparations challenging, optimal flow cell design is extremely important so that peak volume matches detector volume. A well-designed flow cell must strike a balance between the desire to minimize dimensions to avoid degradation in chromatographic resolution and the necessity to maximize the amount of analyte that resides within the V_{obs} so that NMR S/N does not suffer. For stopped-flow data acquisition, the flow cell design should aim

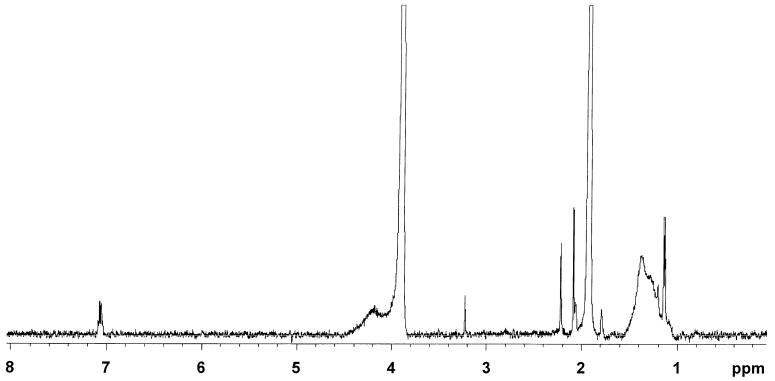

Fig. 4. Stopped-flow NMR spectrum of the impurity peak (peak 3 in Figs. 2A and 3A). Acquisition and processing parameters: SW=5000 Hz, NP=14 976, NT=3200, AT=1.498 s, d1=0.2 s, total NMR experimental time=91 min, LB=1 Hz.

to counteract the drive of diffusion to dilute the peak concentration below a point of diminishing return in terms of S/N per unit time. To determine the effect of diffusion on the signal intensity of a peak that has been positioned within the V_{obs} of the NMR flow cell, NMR data were collected under stopped-flow conditions both shortly after the termination of flow and after a period of 14 h. As shown in Fig. 5, a comparison of integrated peak intensity for the doublet at 0.95 ppm of γ-terpinene demonstrates that ~57% of the original signal intensity remains after 14 h. If the spectra are evaluated with respect to S/N, ~47% of the signal remains after 14 h. Since the probe was not reshimmed during this period, an increase in the full width at half maximum of the resonances in the latter spectrum (e.g., from 6.4 Hz to 7.1 Hz for the peak at 1.60 ppm after applying 1.5 Hz of line broadening) accounted for the differences in the determination of signal degradation by S/N compared to integration. While integral values reflect the extent of diffusional dilution, S/N provides a measure of the overall probe performance for long data collection times. After 14 h, the intensities of both the water and the acetonitrile resonances increase slightly. This sample was prepared in protonated solvent to demonstrate that the cHPLC column could exchange the protonated solvent for the deuterated mobile phase. However, diffusion over the course of many hours increased the concentration of the protonated solvents in the microcoil V_{obs}.

With the current design, a relatively small I.D. (100 μm) capillary feeds into the significantly larger I.D. (700 μm) of the V_{obs}. As such, one end of the flow cell is essentially plugged with respect to diffusion while the other is basically an infinitely long cylinder. Although the data show that the diffusional dilution is not prohibitive for reasonably long NMR experimental times (14 h) for this particular combination of cHPLC column and NMR flow cell, two-dimensional experiments may reveal skewed intensities due to the decreasing concentrations with time. Studies with ''bubble''-type cells

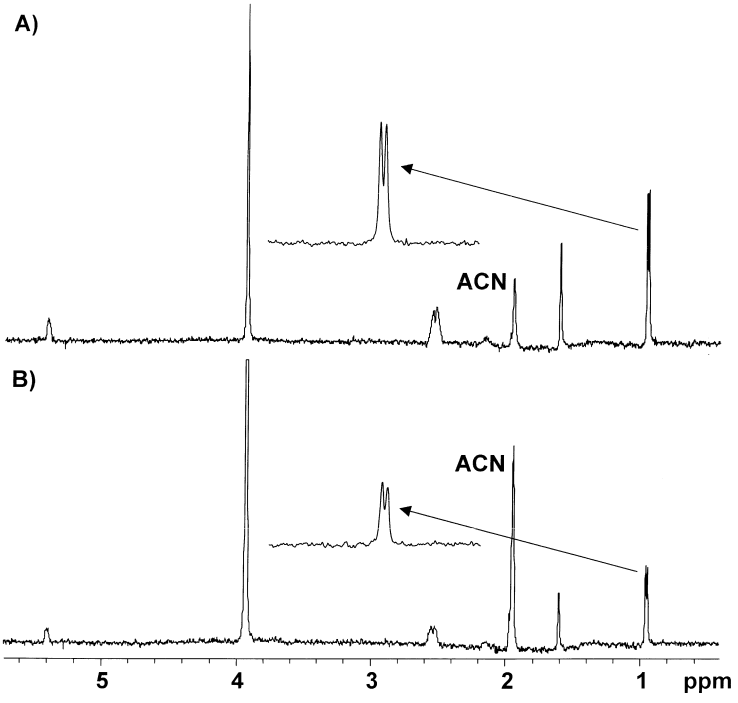

Fig. 5. Stopped-flow NMR spectrum of γ-terpinene. (A) Acquired 7.5 min after terminating the flow. For the doublet at 0.95 ppm, S/N=76, integrated area=1.00. (B) Acquired 14 h after terminating the flow. For the doublet at 0.95 ppm, S/N=36, integrated area=0.57. ~29 nmol (4 μg) injected. Acquisition and processing parameters: SW=3800 Hz, NP=9424, NT=8, AT=1.24 s, total NMR experimental time per spectrum=10 s, LB=1.5 Hz, LN=2 pts. The residual protonated acetonitrile in the mobile phase is labeled as ACN.

are currently underway as an improvement to the current design. The success of Albert and co-workers with these types of flow cells coupled to Helmholtz RF coils appears promising [26,29]. However, optimization of relative dimensions (e.g., wall thickness, length and degree of taper, etc.) for solenoidal RF coils requires further examination so that the flow cell minimizes the effects of diffusion without compromising NMR spectral resolution.

In addition to its strengths in the area of structural elucidation, NMR offers a wide array of diagnostic capabilities which range from pH measurements within bacterial cells [38] to determinations of molecular dispersion within packed chromatographic beds [39].

Within the realm of flow-NMR, the effect of changing mobile phase composition on the spectra is readily monitored. Although commonly implemented with other means of detection, rapid changes in solvent composition for the purposes of faster separations or efficient analyte preconcentration/elution have been largely prohibited for HPLC–NMR. In fact, spectral degradation results whenever a significantly different solvent enters the V_{obs}. As just one example, Fig. 6 illustrates the effect of a 3 μl injection of D_2O–d-ACN (15:85) into a mobile phase consisting of D_2O–d-ACN (10:90). As the injected plug begins to enter the NMR flow cell (V_{obs}~1.1 μl), the coil experiences an increasingly significant solvent gradient across its length. When the plug is centered within the coil, the spectra regain their quality (albeit with shifted resonance frequencies). The spectra again degrade as the plug exits the coil. While the HOD signal shifts downfield by almost 0.20 ppm, the residual protonated acetonitrile signal shifts by only 0.02 ppm. Since the acetonitrile and the water are not affected to a similar degree in terms of frequency shift, the degradation cannot arise simply from a change in magnetic susceptibility within the V_{obs}.

To further test this hypothesis, a mixture of water and acetone-d_6 was prepared to match the magnetic susceptibility (within 1%) of a d-ACN–D_2O (90:10) mobile phase. For a 3 μl injection plug, the water resonance shifted downfield by more than 1 ppm (500 Hz) while the acetonitrile resonance began to shift upfield before fading away and then reappearing as the plug passed through the NMR detector. To isolate the effect of magnetic susceptibility without dramatically changing solvent composition, a 200-nl injection of 100 m*M* $CuSO_4$ in D_2O was made into a D_2O mobile phase. The magnetic susceptibility of 100 m*M* $CuSO_4$ compared to D_2O differs by ~20%. Although the signal broadened substantially, the resonance frequency shifted by only ~5 Hz. In contrast, a 200-nl injection of neat acetone into D_2O caused more significant degradation in spectral resolution as well as a shift of ~17 Hz. Compared to D_2O, acetone differs in magnetic susceptibility by ~35%. Clearly, magnetic susceptibility can play a role in the spectral degradation that accompanies steep solvent gradients across the NMR coil in these

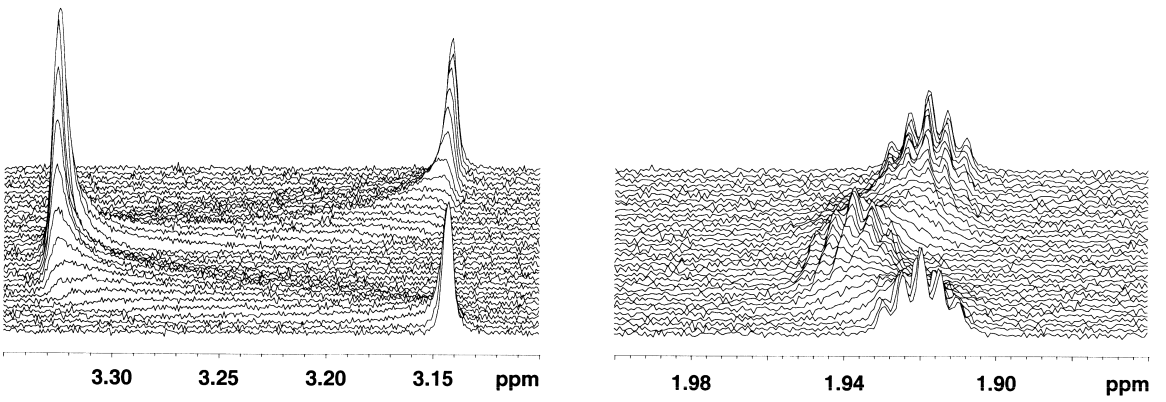

Fig. 6. Stacked plot of NMR spectra that shows the effect of a 3 μl injection of D_2O–d-ACN (15:85) into D_2O–d-ACN (10:90) mobile phase. Flow-rate=3 μl/min. Acquisition and processing parameters: SW=2999.2 Hz, NP=11 968, NT=1, AT= 1.995 s, d1=3 s, total NMR experimental time per spectrum=5 s.

examples. However, shifting resonance frequencies with solvent composition can have an even greater effect on overall spectral quality.

Since resonance frequencies depend to a varying extent on solvent composition [40], smaller NMR probe V_{obs} which would see a narrower range of both solvent composition and magnetic susceptibility for a given flow-rate would allow greater changes in solvent composition per unit time. On the other hand, smaller cells would compromise overall S/N. Clearly, no single NMR flow cell is optimal for all cHPLC–NMR experiments and choices should be made to suit the particular application.

Acknowledgements

It is a pleasure to acknowledge Dr. Dean L. Olson and Dr. James Norcross (MRM Corp.), Dr. Raju Subramanian, Dr. Paul F. Molitor, Andrew M. Wolters, Wayne P. Kelley, and Prof. Cynthia K. Larive (University of Kansas, KS, USA) for technical assistance, useful discussions, and critical evaluation of the manuscript. We appreciate access to the Varian Oxford Instruments Center for Excellence in NMR (VOICE Lab) in the School of Chemical Sciences at the University of Illinois and the use of the cHPLC system from MRM Corp. We gratefully acknowledge financial support from the National Institutes of Health (GM53030), the National Science Foundation (CAREER award to A.G.W.), and a graduate fellowship sponsored by Procter & Gamble (M.E.L.).

References

[1] T. Hirschfeld, Anal. Chem. 52 (1980) 297A.
[2] S. Cohen, B.J. Murphy, Am. Lab. 31 (1999) 28.
[3] H.C. Dorn, J. Gu, D.S. Bethune, R.D. Johnson, C.S. Yannoni, Chem. Phys. Lett. 203 (1993) 549.
[4] G. Navon, Y.Q. Song, T. Room, S. Appelt, R.E. Taylor, A. Pines, Science 271 (1996) 1848.
[5] P.F. Flynn, D.L. Mattiello, H.D.W. Hill, A.J. Wand, J. Am. Chem. Soc. 122 (2000) 4823.
[6] P.J. Hajduk, T. Gerfin, J.-M. Boehlen, M. Häberli, D. Marek, S.W. Fesik, J. Med. Chem. 42 (1999) 2315.
[7] D.J. Russell, C.E. Hadden, C.E. Martin, A.A. Gibson, A.P. Zens, J.L. Carolan, J. Nat. Prod. 63 (2000) 1047.
[8] J.N. Shoolery, Top. Carbon-13 NMR Spectrosc. 3 (1979) 28.
[9] T.M. Barbara, J. Magn. Reson., Ser. A 109 (1994) 265.
[10] C.E. Hadden, G.E. Martin, Magn. Reson. Chem. 37 (1999) 385.
[11] T.L. Peck, R.L. Magin, P.C. Lauterbur, J. Magn. Reson. B 108 (1995) 114.
[12] D.L. Olson, M.E. Lacey, J.V. Sweedler, Anal. Chem. 70 (1998) 257A.
[13] M.E. Lacey, R. Subramanian, D.L. Olson, A.G. Webb, J.V. Sweedler, Chem. Rev. 99 (1999) 3133.
[14] N. Watanabe, E. Niki, Proc. Jpn. Acad., Ser. B 54 (1978) 194.
[15] E. Bayer, K. Albert, M. Nieder, E. Grom, T. Keller, J. Chromatogr. 186 (1979) 497.
[16] D.A. Laude Jr., R.W.-K. Lee, C.L. Wilkins, Anal. Chem. 57 (1985) 1464.
[17] S.H. Smallcombe, S.L. Patt, P.A. Keifer, J. Magn. Reson. 117 (1995) 295.
[18] U.G. Sidelmann, U. Braumann, M. Hofmann, M. Spraul, J.C. Lindon, J.K. Nicholson, S.H. Hansen, Anal. Chem. 69 (1997) 607.
[19] S.C. Bobzin, S. Yang, T.P. Kasten, J. Chromatogr. B 748 (2000) 259.
[20] J.C. Lindon, J.K. Nicholson, I.D. Wilson, J. Chromatogr. B 748 (2000) 233.
[21] N. Wu, T.L. Peck, A.G. Webb, R.L. Magin, J.V. Sweedler, J. Am. Chem. Soc. 116 (1994) 7929.
[22] N. Wu, T.L. Peck, A.G. Webb, R.L. Magin, J.V. Sweedler, Anal. Chem. 66 (1994) 3849.
[23] N. Wu, A. Webb, T.L. Peck, J.V. Sweedler, Anal. Chem. 67 (1995) 3101.
[24] K. Albert, G. Schlotterbeck, L.-H. Tseng, U. Braumann, J. Chromatogr. A 750 (1996) 303.
[25] B. Behnke, G. Schlotterbeck, U. Tallarek, S. Strohschein, L.-H. Tseng, T. Keller, K. Albert, E. Bayer, Anal. Chem. 68 (1996) 1110.
[26] K. Pusecker, J. Schewitz, P. Gfrörer, L.-H. Tseng, K. Albert, E. Bayer, Anal. Chem. 70 (1998) 3280.
[27] R. Subramanian, W.P. Kelley, P.D. Floyd, Z.J. Tan, A.G. Webb, J.V. Sweedler, Anal. Chem. 71 (1999) 5335.
[28] P. Gfrörer, J. Schewitz, K. Pusecker, L.-H. Tseng, K. Albert, E. Bayer, Electrophoresis 20 (1999) 3.
[29] J. Schewitz, K. Pusecker, P. Gfrörer, U. Götz, L.-H. Tseng, K. Albert, E. Bayer, Chromatographia 50 (1999) 333.
[30] J.C. Giddings, Unified Separation Science, Wiley, New York, 1991.
[31] P.S. Meyer, J.C. Dupreez, M.S. Vandyk, Biotechnol. Lett. 16 (1994) 125.
[32] D.M. Beaupre, M. Talpaz, F.C. Marini, R.J. Cristiano, J.A. Roth, Z. Estrov, M. Albitar, M.H. Freedman, R. Kurzrock, Cancer Res. 59 (1999) 2971.
[33] M. Havaux, Trends Plant Sci. 3 (1998) 147.
[34] O. Spring, H. Buschmann, B. Vogler, E.E. Schilling, M. Spraul, M. Hoffmann, Phytochemistry 39 (1995) 609.

[35] D.L. Olson, T.L. Peck, A.G. Webb, R.L. Magin, J.V. Sweedler, Science 270 (1995) 1967.
[36] D. Louden, A. Handley, S. Taylor, E. Lenz, S. Miller, I.D. Wilson, A. Sage, Anal. Chem. 72 (2000) 3922.
[37] L. Griffiths, Magn. Reson. Chem. 35 (1997) 257.
[38] B.A. Lawrence, J. Polse, A. DePina, M.M. Allen, N.H. Kolodny, Curr. Microbiol. 34 (1997) 280.
[39] U. Tallarek, E. Bayer, G. Guiochon, J. Am. Chem. Soc. 120 (1998) 1494.
[40] H.E. Gottlieb, V. Kotlyar, A. Nudelman, J. Org. Chem. 62 (1997) 7512.